

Article

# On the Solitary Waves and Nonlinear Oscillations to the Fractional Schrödinger–KdV Equation in the Framework of the Caputo Operator

Saima Noor <sup>1,\*</sup>, Badriah M. Alotaibi <sup>2</sup>, Rasool Shah <sup>3</sup>, Sherif M. E. Ismaeel <sup>4,5</sup> and Samir A. El-Tantawy <sup>6,7,†</sup><sup>1</sup> Department of Basic Sciences, Preparatory Year Deanship, King Faisal University, Al Ahsa 31982, Saudi Arabia<sup>2</sup> Department of Physics, College of Science, Princess Nourah bint Abdulrahman University, P.O. Box 84428, Riyadh 11671, Saudi Arabia<sup>3</sup> Department of Mathematics, Abdul Wali Khan University, Mardan 23200, Pakistan<sup>4</sup> Department of Physics, College of Science and Humanities in Al-Kharj, Prince Sattam bin Abdulaziz University, Al-Kharj 11942, Saudi Arabia<sup>5</sup> Department of Physics, Faculty of Science, Ain Shams University, Cairo 11566, Egypt<sup>6</sup> Department of Physics, Faculty of Science, Port Said University, Port Said 42521, Egypt; tantawy@sci.psu.edu.eg<sup>7</sup> Research Center for Physics (RCP), Department of Physics, Faculty of Science and Arts, Al-Mikhwah, Al-Baha University, Al-Baha 1988, Saudi Arabia

\* Correspondence: snoor@kfu.edu.sa

† This author participated in the largest part of the discussion and analysis of the results and the review of the whole manuscript.

**Abstract:** The fractional Schrödinger–Korteweg-de Vries (S-KdV) equation is an important mathematical model that incorporates the nonlinear dynamics of the KdV equation with the quantum mechanical effects described by the Schrödinger equation. Motivated by the several applications of the mentioned evolution equation, in this investigation, the Laplace residual power series method (LRPSM) is employed to analyze the fractional S-KdV equation in the framework of the Caputo operator. By incorporating both the Caputo operator and fractional derivatives into the mentioned evolution equation, we can account for memory effects and non-local behavior. The LRPSM is a powerful analytical technique for the solution of fractional differential equations and therefore it is adapted in our current study. In this study, we prove that the combination of the residual power series expansion with the Laplace transform yields precise and efficient solutions. Moreover, we investigate the behavior and properties of the (un)symmetric solutions to the fractional S-KdV equation using extensive numerical simulations and by considering various fractional orders and initial fractional values. The results contribute to the greater comprehension of the interplay between quantum mechanics and nonlinear dynamics in fractional systems and shed light on wave phenomena and symmetry soliton solutions in such equations. In addition, the proposed method successfully solves fractional differential equations with the Caputo operator, providing a valuable computational instrument for the analysis of complex physical systems. Moreover, the obtained results can describe many of the mysteries associated with the mechanism of nonlinear wave propagation in plasma physics.

**Keywords:** Laplace transform; fractional Schrödinger–KdV equation; residual power series; Caputo operator



**Citation:** Noor, S.; Alotaibi, B.M.; Shah, R.; Ismaeel, S.M.E.; El-Tantawy, S.A. On the Solitary Waves and Nonlinear Oscillations to the Fractional Schrödinger–KdV Equation in the Framework of the Caputo Operator. *Symmetry* **2023**, *15*, 1616. <https://doi.org/10.3390/sym15081616>

Academic Editors: Józef Banaś, Agnieszka Chlebowicz, Beata Rzepka and Palle E.T. Jorgensen

Received: 9 July 2023

Revised: 9 August 2023

Accepted: 11 August 2023

Published: 21 August 2023



**Copyright:** © 2023 by the authors. Licensee MDPI, Basel, Switzerland. This article is an open access article distributed under the terms and conditions of the Creative Commons Attribution (CC BY) license (<https://creativecommons.org/licenses/by/4.0/>).

## 1. Introduction

Fractional calculus (FC) has emerged as a powerful mathematical tool to describe phenomena involving non-local and memory-dependent effects. It has many applications in various scientific disciplines, from physics and engineering to economics and biology. The theory and applications of fractional differential equations (DEs) have been extensively studied and developed over the years, contributing to a deeper understanding of complex systems. Many papers have been published on this topic due to its importance in the

in-depth explanation of many mysterious phenomena in various physics problems [1,2]. Some of the most important books published on this subject are the books of Kilbas et al. [3] and Baleanu et al. [4], which provide comprehensive insights into the application and theory of fractional DEs. These books serve as valuable references for researchers and practitioners seeking to explore the interdisciplinary nature of FC. The work of Caputo [5], and Riemann [6] laid the foundations for the development of FC, introducing fundamental concepts and mathematical techniques.

The introduction of fractional derivatives by Liouville [7] paved the way for further advancements in the field. The works of Podlubny [8] and Miller and Ross [9] delved into the theory of FC and provided detailed explanations of fractional DEs. These resources have been crucial in establishing the theoretical framework for the study of fractional systems. The practical applications of FC are wide-ranging. For instance, Li et al. [10] applied fractional diffusion equations to signal smoothing, demonstrating their effectiveness in signal processing. Lin [11] contributed to the concept of global existence and chaos control in fractional DEs, shedding light on the behavior of complex dynamical systems. Additionally, Veerasha et al. [12] used a modified homotopy analysis transform method to solve a smoking epidemic model of fractional order, highlighting the relevance of FC in modeling real-world phenomena [13–19].

The nonlinear Schrödinger equation (NLSE) is a fundamental equation in nonlinear optics, quantum mechanics and the physics of plasma, describing the dynamics of modulated wave propagation in nonlinear media. It is a partial DE incorporating dispersion and nonlinear effects, allowing for the study of nonlinear phenomena such as modulated envelope solitons, rogue waves and breathers, as well as the study of the modulational instability of modulated nonlinear wave [20–25]. The NLSE can be derived from the linear Schrödinger equation by including a nonlinear term that accounts for the interaction between the wave and the medium. This nonlinear term is typically expressed as a power law function of the wave intensity or amplitude, representing the intensity-dependent refractive index of the medium. As a result, the NLSE captures the intricate interplay between linear dispersion and nonlinear self-interaction [26,27].

The nonlinear classical Schrödinger-KdV equation is defined as [28,29]

$$\begin{aligned} ip_t &= p_{qq} + pq, \\ w_t &= -6ww_q - w_{qqq} + (|p|^2)_q \end{aligned} \quad (1)$$

where  $i = \sqrt{-1}$ . Adopting  $p = u + iv$  allows us to separate Equation (1) into real and imaginary parts. In this framework, the following  $(1 + 1)$ -dimensional tripled system can be realized:

$$\begin{aligned} u_t - v_{qq} - vw &= 0, \\ v_t + u_{qq} + uw &= 0, \\ w_t + 6ww_q + w_{qqq} - 2uu_q - 2vv_q &= 0. \end{aligned} \quad (2)$$

The NLSE has found broad applications in different fields of physics, including nonlinear optics, fiber optics, condensed matter physics, plasma physics and Bose–Einstein condensates. It provides a versatile framework for the study of phenomena such as optical solitons, which are self-sustaining, localized wave packets that retain their shape and velocity during propagation. Solitons are particularly interesting due to their robustness and potential applications in high-speed communication systems. The NLSE exhibits various solutions, ranging from simple plane waves to complex localized structures such as bright solitons, dark solitons, rogue waves and breathers [20–25]. These solutions arise due to the delicate balance between dispersion, which tends to be associated with wave propagation, and nonlinearity, which counteracts the spreading by self-focusing or self-defocusing effects. Understanding the dynamics and properties of solutions to the NLSE is crucial in advancing our knowledge of nonlinear wave phenomena. The study of the NLSE involves

various mathematical and computational techniques, including analytical methods, numerical simulations and experimental investigations. Researchers continue to explore the NLSE and its extensions to gain deeper insights into nonlinear wave propagation and its applications in diverse fields [26,27].

Some notable contributions include the following. Triki and Biswas (2011) investigated dark solitons for a generalized NLSE with a parabolic law and dual power nonlinearity, providing insights into the soliton dynamics governed by these specific nonlinear terms [30]. Zhang and Si (2010) presented new soliton and periodic solutions for the (1 + 2)-dimensional NLSE with dual power nonlinearity, shedding light on the existence and characteristics of these solutions [31]. Biswas (2001) examined the perturbation of solitons due to power law nonlinearity, revealing the effects of nonlinear terms on soliton structures [32]. Bronski et al. (2001) investigated the cubic NLSE with a periodic potential and its implications for condensed matter systems in standing waves [33]. Nore et al. (1993) performed a numerical study of hydrodynamics using the NLSE, highlighting the applicability of this equation in describing fluid dynamics and turbulence [34]. Eslami and Mirzazadeh (2013) investigated the topological 1-soliton solutions of the NLSE with dual power nonlinearity in optical fibers, providing insights into the behavior of soliton-like structures in these systems [35]. The main objective of this investigation is to apply the Laplace residual power series method (LRPSM) [36] for the analysis of the fractional S-KdV model in the framework of the Caputo operator. In addition, a comparison between the obtained approximations and the exact solutions for the integer case is performed. Additionally, we demonstrate that the obtained approximations are distinguished by high accuracy and are more stable against the large space-time domain.

The rest of the current work is divided into the following sections. In Section 2, we briefly describe the basic definitions related to the suggested method. The general implementation of the suggested technique is described in Section 3. Some numerical applications are introduced in Section 4. In Section 5, the obtained results are briefly summarized.

### 2. Basic Definitions

**Definition 1.** The Caputo fractional derivative of a function  $\mu(q, t)$  of order  $\delta$  is defined as [37]

$${}^C D_t^\delta \mu(q, t) = J_t^{m-\delta} \mu^m(q, t), \quad m - 1 < \delta \leq m, \quad t > 0. \tag{3}$$

where  $m \in \mathbb{N}$  and  $J_t^\delta$  indicates the fractional integral Riemann–Liouville (RL) of  $\mu(q, t)$  of order  $\delta$ , which is given by

$$J_t^\delta \mu(q, t) = \frac{1}{\Gamma(\delta)} \int_0^t (t - \rho)^{\delta-1} \mu(q, \rho) d\rho. \tag{4}$$

**Definition 2.** The Laplace transform (LT) of  $\mu(q, t)$  is defined by [38]

$$\mu(q, s) = \mathcal{L}_t[\mu(q, t)] = \int_0^\infty e^{-st} \mu(q, t) dt, \quad s > \delta, \tag{5}$$

where the inverse of LT is given by

$$\mu(q, t) = \mathcal{L}_t^{-1}[\mu(q, s)] = \int_{l-i\infty}^{l+i\infty} e^{st} \mu(q, s) ds, \quad l = \text{Re}(s) > l_0. \tag{6}$$

**Lemma 1.** Let  $u(q, t)$  be a piecewise continuous function and  $U(q, s) = \mathcal{L}_t[u(q, t)]$  be its LT with respect to time.

1.  $\mathcal{L}_t[J_t^\delta u(q, t)] = \frac{U(q, s)}{s^\delta}, \quad \delta > 0.$
2.  $\mathcal{L}_t[D_t^\delta u(q, t)] = s^\delta U(q, s) - \sum_{\kappa=0}^{m-1} s^{\delta-\kappa-1} u^\kappa(q, 0), \quad m - 1 < \delta \leq m.$
3.  $\mathcal{L}_t[D_t^{n\delta} u(q, t)] = s^{n\delta} U(q, s) - \sum_{\kappa=0}^{n-1} s^{(n-\kappa)\delta-1} D_t^{\kappa\delta} u(q, 0), \quad 0 < \delta \leq 1.$

**Proof.** More details of this proof can be found in refs. [38,39].  $\square$

**Theorem 1.** Let  $u(\varrho, t)$  be a piecewise continue term on  $I \times [0, \infty)$  with exponential order  $\varrho$ . Suppose that the fractional order of the function  $U(\varrho, s) = \mathcal{L}_t[u(\varrho, t)]$  is defined by [40]

$$U(\varrho, s) = \sum_{n=0}^{\infty} \frac{f_n(\varrho)}{s^{n\delta+1}}, 0 < \delta \leq 1, \varrho \in I, s > \varrho. \tag{7}$$

Then,  $f_n(\varrho) = D_i^{n\delta}u(\varrho, 0)$ .

### 3. General Implementation

Consider the following fractional partial DE:

$$D_i^\delta \mu(\varrho, t) + N[\mu(\varrho, t)] + R[\mu(\varrho, t)] = 0, \text{ where } 0 < \delta \leq 1. \tag{8}$$

This is subjected to initial condition (IC)

$$\mu(\varrho, t) = f_0(\varrho). \tag{9}$$

Applying LT to Equation (8) and using Equation (9), we obtain

$$\mu(\varrho, s) - \frac{f_0(\varrho, s)}{s} + \frac{1}{s^\delta} \mathcal{L}_t [N[\mathcal{L}_t^{-1}[\mu(\varrho, s)]] + R[\mu(\varrho, s)]] = 0. \tag{10}$$

Suppose that the result of Equation (10) is defined as

$$\mu(\varrho, s) = \sum_{n=0}^{\infty} \frac{f_n(\varrho)}{s^{n\delta+1}}, \tag{11}$$

and the  $\kappa$ th-truncated term series reads

$$\mu(\varrho, s) = \frac{f_0(\varrho)}{s} + \sum_{n=1}^{\kappa} \frac{f_n(\varrho)}{s^{n\delta+1}}. \tag{12}$$

The Laplace residual functions read [41]

$$\mathcal{L}_t Res(\varrho, s) = \mu(\varrho, s) - \frac{f_0(\varrho)}{s} + \frac{1}{s^\delta} \mathcal{L}_t [N[\mathcal{L}_t^{-1}[\mu(\varrho, s)]] + R[\mu(\varrho, s)]]. \tag{13}$$

Moreover, the  $\kappa$ th-LRFs read

$$\mathcal{L}_t Res_\kappa(\varrho, s) = \mu_\kappa(\varrho, s) - \frac{f_0(\varrho)}{s} + \frac{1}{s^\delta} \mathcal{L}_t [N[\mathcal{L}_t^{-1}[\mu_\kappa(\varrho, s)]] + R[\mu_\kappa(\varrho, s)]]. \tag{14}$$

The LRPSM features are listed below to illustrate the following points:

- $\mathcal{L}_t Res(\varrho, s) = 0$  and  $\lim_{j \rightarrow \infty} \mathcal{L}_t Res_\kappa(\varrho, s) = \mathcal{L}_t Res_\mu(\varrho, s)$  for each  $s > 0$ ,
- $\lim_{s \rightarrow \infty} s \mathcal{L}_t Res_\mu(\varrho, s) = 0 \Rightarrow \lim_{s \rightarrow \infty} s \mathcal{L}_t Res_{\mu, \kappa}(\varrho, s) = 0$ ,
- $\lim_{s \rightarrow \infty} s^{\kappa\delta+1} \mathcal{L}_t Res_{\mu, \kappa}(\varrho, s) = \lim_{s \rightarrow \infty} s^{\kappa\delta+1} \mathcal{L}_t Res_{u, \kappa}(\varrho, s) = 0, 0 < \delta \leq 1, \kappa = 1, 2, 3, \dots$ .

The recursive solution for the calculation of the coefficients using  $f_n(\varrho)$  is obtained by solving the following system of equations [41]:

$$\lim_{s \rightarrow \infty} s^{\kappa\delta+1} \mathcal{L}_t Res_{\mu, \kappa}(\delta, s) = 0, \kappa = 1, 2, \dots \tag{15}$$

Finally, we take the inverse of LT in Equation (11), to obtain the  $\kappa$ th analytic solution of  $\mu_\kappa(\varrho, t)$ .

### 4. Numerical Results

#### Example

Let us analyze the following fractional nonlinear system of S-KdV models [42]:

$$\begin{aligned}
 D_t^\delta u(\varrho, t) - \partial_{\varrho\varrho} v(\varrho, t) - v(\varrho, t)w(\varrho, t) &= 0, \quad \text{where } , 0 < \delta \leq 1 \\
 D_t^\delta v(\varrho, t) + \partial_{\varrho\varrho} u(\varrho, t) + u(\varrho, t)w(\varrho, t) &= 0, \\
 D_t^\delta w(\varrho, t) + 6w(\varrho, t)\partial_{\varrho} w(\varrho, t) + \partial_{\varrho\varrho\varrho} w(\varrho, t) - 2u(\varrho, t)\partial_{\varrho} u(\varrho, t) - 2v(\varrho, t)\partial_{\varrho} v(\varrho, t) &= 0,
 \end{aligned}
 \tag{16}$$

which are subjected to the following ICs [42]:

$$\begin{aligned}
 u(\varrho, 0) &= \tanh(\varrho)\cos(\varrho), \\
 v(\varrho, 0) &= \tanh(\varrho)\sin(\varrho), \\
 w(\varrho, 0) &= \frac{7}{8} - 2\tanh^2(\varrho).
 \end{aligned}
 \tag{17}$$

Applying LT to Equation (16) yields

$$\begin{aligned}
 s^\delta \mathcal{L}[u(\varrho, t)] - s^{\delta-1}u(\varrho, 0) - \mathcal{L}[\partial_{\varrho\varrho} v(\varrho, t)] - \mathcal{L}[v(\varrho, t)w(\varrho, t)] &= 0, \\
 s^\delta \mathcal{L}[v(\varrho, t)] - s^{\delta-1}v(\varrho, 0) + \mathcal{L}[\partial_{\varrho\varrho} u(\varrho, t)] + \mathcal{L}[u(\varrho, t)w(\varrho, t)] &= 0, \\
 s^\delta \mathcal{L}[w(\varrho, t)] - s^{\delta-1}w(\varrho, 0) + 6\mathcal{L}[w(\varrho, t)\partial_{\varrho} w(\varrho, t)] + \mathcal{L}[\partial_{\varrho\varrho\varrho} w(\varrho, t)] \\
 - 2\mathcal{L}[u(\varrho, t)\partial_{\varrho} u(\varrho, t)] - 2\mathcal{L}[v(\varrho, t)\partial_{\varrho} v(\varrho, t)] &= 0,
 \end{aligned}
 \tag{18}$$

where  $\mathcal{L}[u(\varrho, t)] = u(\varrho, s)$ ,  $\mathcal{L}[v(\varrho, t)] = v(\varrho, s)$  and  $\mathcal{L}[w(\varrho, t)] = w(\varrho, s)$ . Using Equation (17) in Equation (18) and dividing the obtained results by  $s^\delta$ , we have

$$\begin{aligned}
 u(\varrho, s) - \frac{\tanh(\varrho)\cos(\varrho)}{s} - \frac{1}{s^\delta}\partial_{\varrho\varrho} v(\varrho, s) - \frac{1}{s^\delta}\mathcal{L}[\mathcal{L}^{-1}[v(\varrho, s)]\mathcal{L}^{-1}[w(\varrho, s)]] &= 0, \\
 v(\varrho, s) - \frac{\tanh(\varrho)\sin(\varrho)}{s} + \frac{1}{s^\delta}\partial_{\varrho\varrho} u(\varrho, s) + \frac{1}{s^\delta}\mathcal{L}[\mathcal{L}^{-1}[u(\varrho, s)]\mathcal{L}^{-1}[w(\varrho, s)]] &= 0, \\
 w(\varrho, s) - \frac{\frac{7}{8} - 2\tanh^2(\varrho)}{s} + \frac{6}{s^\delta}\mathcal{L}[\mathcal{L}^{-1}[w(\varrho, s)]\mathcal{L}^{-1}[\partial_{\varrho} w(\varrho, s)]] + \frac{1}{s^\delta}\partial_{\varrho\varrho\varrho} w(\varrho, s) \\
 - \frac{2}{s^\delta}\mathcal{L}[\mathcal{L}^{-1}[u(\varrho, s)]\mathcal{L}^{-1}[\partial_{\varrho} u(\varrho, s)]] - \frac{2}{s^\delta}\mathcal{L}[\mathcal{L}^{-1}[v(\varrho, s)]\mathcal{L}^{-1}[\partial_{\varrho} v(\varrho, s)]] &= 0.
 \end{aligned}
 \tag{19}$$

The  $\kappa$ th-truncated term series read

$$\begin{aligned}
 u(\varrho, s) &= \frac{f_0(\varrho, s)}{s} + \sum_{n=1}^{\kappa} \frac{f_n(\varrho, s)}{s^{n\delta+1}}, n = 1, 2, 3, 4 \dots \\
 v(\varrho, s) &= \frac{g_0(\varrho, s)}{s} + \sum_{n=1}^{\kappa} \frac{g_n(\varrho, s)}{s^{n\delta+1}}, \\
 w(\varrho, s) &= \frac{h_0(\varrho, s)}{s} + \sum_{n=1}^{\kappa} \frac{h_n(\varrho, s)}{s^{n\delta+1}}.
 \end{aligned}
 \tag{20}$$

Here,  $f_0(\varrho, s) = u(\varrho, 0) = \tanh(\varrho)\cos(\varrho)$ ,  $g_0(\varrho, s) = v(\varrho, 0) = \tanh(\varrho)\sin(\varrho)$  and  $h_0(\varrho, s) = w(\varrho, 0) = \frac{7}{8} - 2\tanh^2(\varrho)$

$$\begin{aligned}
 u(\varrho, s) &= \frac{\tanh(\varrho)\cos(\varrho)}{s} + \sum_{n=1}^{\kappa} \frac{f_n(\varrho, s)}{s^{n\delta+1}}, \\
 v(\varrho, s) &= \frac{\tanh(\varrho)\sin(\varrho)}{s} + \sum_{n=1}^{\kappa} \frac{g_n(\varrho, s)}{s^{n\delta+1}}, \\
 w(\varrho, s) &= \frac{\frac{7}{8} - \tanh^2(\varrho)}{s} + \sum_{n=1}^{\kappa} \frac{h_n(\varrho, s)}{s^{n\delta+1}}, \\
 \kappa &= 1, 2, 3, 4 \dots
 \end{aligned}
 \tag{21}$$

The residual Laplace function is given by

$$\begin{aligned}
 \mathcal{L}_t Res_u(\varrho, s) &= u(\varrho, s) - \frac{\tanh(\varrho)\cos(\varrho)}{s} - \frac{1}{s^\delta} \partial_{\varrho\varrho} v(\varrho, s) - \frac{1}{s^\delta} \mathcal{L}[\mathcal{L}^{-1}[v(\varrho, s)]\mathcal{L}^{-1}[w(\varrho, s)]], \\
 \mathcal{L}_t Res_v(\varrho, s) &= v(\varrho, s) - \frac{\tanh(\varrho)\sin(\varrho)}{s} + \frac{1}{s^\delta} \partial_{\varrho\varrho} u(\varrho, s) + \frac{1}{s^\delta} \mathcal{L}[\mathcal{L}^{-1}[u(\varrho, s)]\mathcal{L}^{-1}[w(\varrho, s)]], \\
 \mathcal{L}_t Res_w(\varrho, s) &= w(\varrho, s) - \frac{\frac{7}{8} - 2\tanh^2(\varrho)}{s} + \frac{6}{s^\delta} \mathcal{L}[\mathcal{L}^{-1}[w(\varrho, s)]\mathcal{L}^{-1}[\partial_{\varrho} w(\varrho, s)]] + \frac{1}{s^\delta} \partial_{\varrho\varrho} w(\varrho, s) \\
 &\quad - \frac{2}{s^\delta} \mathcal{L}[\mathcal{L}^{-1}[u(\varrho, s)]\mathcal{L}^{-1}[\partial_{\varrho} u(\varrho, s)]] - \frac{2}{s^\delta} \mathcal{L}[\mathcal{L}^{-1}[v(\varrho, s)]\mathcal{L}^{-1}[\partial_{\varrho} v(\varrho, s)]].
 \end{aligned}
 \tag{22}$$

According to the LRPS methodology, the  $\kappa$ th-LRFs read

$$\begin{aligned}
 \mathcal{L}_t Res_{u,\kappa}(\varrho, s) &= u_\kappa(\varrho, s) - \frac{\tanh(\varrho)\cos(\varrho)}{s} - \frac{1}{s^\delta} \partial_{\varrho\varrho} v_\kappa(\varrho, s) - \frac{1}{s^\delta} \mathcal{L}[\mathcal{L}^{-1}[v_\kappa(\varrho, s)]\mathcal{L}^{-1}[w_\kappa(\varrho, s)]], \\
 \mathcal{L}_t Res_{v,\kappa}(\varrho, s) &= v_\kappa(\varrho, s) - \frac{\tanh(\varrho)\sin(\varrho)}{s} + \frac{1}{s^\delta} \partial_{\varrho\varrho} u_\kappa(\varrho, s) + \frac{1}{s^\delta} \mathcal{L}[\mathcal{L}^{-1}[u_\kappa(\varrho, s)]\mathcal{L}^{-1}[w_\kappa(\varrho, s)]], \\
 \mathcal{L}_t Res_{w,\kappa}(\varrho, s) &= w_\kappa(\varrho, s) - \frac{\frac{7}{8} - 2\tanh^2(\varrho)}{s} + \frac{6}{s^\delta} \mathcal{L}[\mathcal{L}^{-1}[w_\kappa(\varrho, s)]\mathcal{L}^{-1}[\partial_{\varrho} w_\kappa(\varrho, s)]] + \frac{1}{s^\delta} \partial_{\varrho\varrho} w_\kappa(\varrho, s) \\
 &\quad - \frac{2}{s^\delta} \mathcal{L}[\mathcal{L}^{-1}[u_\kappa(\varrho, s)]\mathcal{L}^{-1}[\partial_{\varrho} u_\kappa(\varrho, s)]] - \frac{2}{s^\delta} \mathcal{L}[\mathcal{L}^{-1}[v_\kappa(\varrho, s)]\mathcal{L}^{-1}[\partial_{\varrho} v_\kappa(\varrho, s)]].
 \end{aligned}
 \tag{23}$$

Now, we can calculate  $f_\kappa(\varrho, s)$ ,  $g_\kappa(\varrho, s)$  and  $h_\kappa(\varrho, s)$   $\kappa = 1, 2, 3, \dots$ , by substituting the  $\kappa$ th-truncated series of Equation (21) into the  $\kappa$ th residual Laplace term in Equation (23), and we then multiply the solution by  $s^{\kappa\delta+1}$  and solve recursively the link  $\lim_{s \rightarrow \infty} (s^{\kappa\delta+1} \mathcal{L}_t Res_{u,\kappa}(\varrho, s)) = 0$ ,  $\lim_{s \rightarrow \infty} (s^{\kappa\delta+1} \mathcal{L}_t Res_{v,\kappa}(\varrho, s)) = 0$ , and  $\lim_{s \rightarrow \infty} (s^{\kappa\delta+1} \mathcal{L}_t Res_{w,\kappa}(\varrho, s)) = 0$   $\kappa = 1, 2, 3, \dots$ . The first few terms are defined by

$$\begin{aligned}
 f_1(\varrho, s) &= 2 \cos(\varrho)\operatorname{sech}^2(\varrho) - \frac{17}{8} \sin(\varrho) \tanh(\varrho), \\
 g_1(\varrho, s) &= \frac{17}{8} \cos(\varrho) \tanh(\varrho) + 2 \sin(\varrho)\operatorname{sech}^2(\varrho), \\
 h_1(\varrho, s) &= \tanh(\varrho) \left( -32\operatorname{sech}^4(\varrho) + \sin(2\varrho) \tanh(\varrho) + 2\operatorname{sech}^2(\varrho) (\sin^2(\varrho) + 8 \tanh^2(\varrho)) \right), \\
 f_2(\varrho, s) &= \sin(\varrho) \sin(2\varrho) \tanh^3(\varrho) - \frac{17}{4} \cos(\varrho) \tanh^3(\varrho) - \frac{17}{64} \cos(\varrho) \tanh(\varrho) - \\
 &\quad 2 \sin(\varrho) (9 \cosh(2\varrho) - 7)\operatorname{sech}^6(\varrho) + \frac{1}{4} \operatorname{sech}^2(\varrho) (-18 \sin(\varrho) + 8 \sin(\varrho) (\sin^2(\varrho) + \\
 &\quad 2) \tanh^2(\varrho) + 64 \sin(\varrho) \tanh^4(\varrho) - 49 \cos(\varrho) \tanh(\varrho)), \\
 g_2(\varrho, s) &= -\frac{1}{64} \tanh(\varrho) (17 \sin(\varrho) + 16(19 \sin(\varrho) + 2 \sin(3\varrho)) \tanh^2(\varrho)) + 2 \cos(\varrho) (9 \cosh(2\varrho) \\
 &\quad - 7)\operatorname{sech}^6(\varrho) - \frac{1}{4} \operatorname{sech}^2(\varrho) (-18 \cos(\varrho) + 49 \sin(\varrho) \tanh(\varrho) + 64 \cos(\varrho) \tanh^4(\varrho) - 2(\cos(3\varrho) \\
 &\quad - 9 \cos(\varrho)) \tanh^2(\varrho)),
 \end{aligned}
 \tag{24}$$

We place the value of  $f_\kappa(\varrho, s)$ ,  $g_\kappa(\varrho, s)$  and  $h_\kappa(\varrho, s)$   $\kappa = 1, 2, 3, \dots$ , in Equation (21), and we obtain

$$\begin{aligned}
 u(\varrho, s) &= \frac{\tanh(\varrho)\cos(\varrho)}{s} + \frac{1}{s^{\delta+1}} \left( 2\cos(\varrho)\operatorname{sech}^2(\varrho) - \frac{17}{8}\sin(\varrho)\tanh(\varrho) \right) + \\
 &\frac{1}{s^{2\delta+1}} \left( \sin(\varrho)\sin(2\varrho)\tanh^3(\varrho) - \frac{17}{4}\cos(\varrho)\tanh^3(\varrho) - \frac{17}{64}\cos(\varrho)\tanh(\varrho) - \right. \\
 &2\sin(\varrho)(9\cosh(2\varrho) - 7)\operatorname{sech}^6(\varrho) + \frac{1}{4}\operatorname{sech}^2(\varrho)(-18\sin(\varrho) + 8\sin(\varrho)(\sin^2(\varrho) \\
 &\left. + 2)\tanh^2(\varrho) + 64\sin(\varrho)\tanh^4(\varrho) - 49\cos(\varrho)\tanh(\varrho)) \right) + \dots \\
 v(\varrho, s) &= \frac{\tanh(\varrho)\sin(\varrho)}{s} + \frac{1}{s^{\delta+1}} \left( \frac{17}{8}\cos(\varrho)\tanh(\varrho) + 2\sin(\varrho)\operatorname{sech}^2(\varrho) \right) + \\
 &\frac{1}{s^{2\delta+1}} \left( -\frac{1}{64}\tanh(\varrho)(17\sin(\varrho) + 16(19\sin(\varrho) + 2\sin(3\varrho))\tanh^2(\varrho)) + \right. \\
 &2\cos(\varrho)(9\cosh(2\varrho) - 7)\operatorname{sech}^6(\varrho) - \frac{1}{4}\operatorname{sech}^2(\varrho)(-18\cos(\varrho) + 49\sin(\varrho)\tanh(\varrho) \\
 &\left. + 64\cos(\varrho)\tanh^4(\varrho) - 2(\cos(3\varrho) - 9\cos(\varrho))\tanh^2(\varrho)) \right) + \dots, \\
 w(\varrho, s) &= \frac{\frac{7}{8} - 2\tanh^2(\varrho)}{s} + \frac{1}{s^{\delta+1}} \left( \tanh(\varrho)(-32\operatorname{sech}^4(\varrho) + \sin(2\varrho)\tanh(\varrho) + \right. \\
 &\left. 2\operatorname{sech}^2(\varrho)(\sin^2(\varrho) + 8\tanh^2(\varrho))) \right) + \dots
 \end{aligned}
 \tag{25}$$

Applying the inverse LT, we obtain

$$\begin{aligned}
 v(\varrho, t) &= \cos(\varrho)\tanh(\varrho) - \frac{17\cos(\varrho)\tanh^3(\varrho)t^{2\delta}}{4\Gamma(2\delta+1)} - \frac{17\cos(\varrho)\tanh(\varrho)t^{2\delta}}{64\Gamma(2\delta+1)} + \frac{\sin(\varrho)\sin(2\varrho)\tanh^3(\varrho)t^{2\delta}}{\Gamma(2\delta+1)} + \\
 &\frac{14\sin(\varrho)\operatorname{sech}^6(\varrho)t^{2\delta}}{\Gamma(2\delta+1)} - \frac{9\sin(\varrho)\operatorname{sech}^2(\varrho)t^{2\delta}}{2\Gamma(2\delta+1)} - \frac{49\cos(\varrho)\tanh(\varrho)\operatorname{sech}^2(\varrho)t^{2\delta}}{4\Gamma(2\delta+1)} - \frac{18\sin(\varrho)\cosh(2\varrho)\operatorname{sech}^6(\varrho)t^{2\delta}}{\Gamma(2\delta+1)} \\
 &+ \frac{2\sin^3(\varrho)\tanh^2(\varrho)\operatorname{sech}^2(\varrho)t^{2\delta}}{\Gamma(2\delta+1)} + \frac{16\sin(\varrho)\tanh^4(\varrho)\operatorname{sech}^2(\varrho)t^{2\delta}}{\Gamma(2\delta+1)} + \frac{4\sin(\varrho)\tanh^2(\varrho)\operatorname{sech}^2(\varrho)t^{2\delta}}{\Gamma(2\delta+1)} \\
 &+ \frac{2\cos(\varrho)\operatorname{sech}^2(\varrho)t^\delta}{\Gamma(\delta+1)} - \frac{17\sin(\varrho)\tanh(\varrho)t^\delta}{8\Gamma(\delta+1)} + \dots, \\
 v(\varrho, t) &= \sin(\varrho)\tanh(\varrho) - \frac{14\cos(\varrho)\operatorname{sech}^6(\varrho)t^{2\delta}}{\Gamma(2\delta+1)} + \frac{9\cos(\varrho)\operatorname{sech}^2(\varrho)t^{2\delta}}{2\Gamma(2\delta+1)} - \frac{\sin(3\varrho)\tanh^3(\varrho)t^{2\delta}}{2\Gamma(2\delta+1)} - \\
 &\frac{19\sin(\varrho)\tanh^3(\varrho)t^{2\delta}}{4\Gamma(2\delta+1)} - \frac{17\sin(\varrho)\tanh(\varrho)t^{2\delta}}{64\Gamma(2\delta+1)} + \frac{18\cos(\varrho)\cosh(2\varrho)\operatorname{sech}^6(\varrho)t^{2\delta}}{\Gamma(2\delta+1)} \\
 &- \frac{16\cos(\varrho)\tanh^4(\varrho)\operatorname{sech}^2(\varrho)t^{2\delta}}{\Gamma(2\delta+1)} + \frac{\cos(3\varrho)\tanh^2(\varrho)\operatorname{sech}^2(\varrho)t^{2\delta}}{2\Gamma(2\delta+1)} - \frac{9\cos(\varrho)\tanh^2(\varrho)\operatorname{sech}^2(\varrho)t^{2\delta}}{2\Gamma(2\delta+1)} \\
 &- \frac{49\sin(\varrho)\tanh(\varrho)\operatorname{sech}^2(\varrho)t^{2\delta}}{4\Gamma(2\delta+1)} + \frac{17\cos(\varrho)\tanh(\varrho)t^\delta}{8\Gamma(\delta+1)} + \frac{2\sin(\varrho)\operatorname{sech}^2(\varrho)t^\delta}{\Gamma(\delta+1)} + \dots, \\
 w(\varrho, t) &= -2\tanh^2(\varrho) + \frac{\sin(2\varrho)\tanh^2(\varrho)t^\delta}{\Gamma(\delta+1)} - \frac{32\tanh(\varrho)\operatorname{sech}^4(\varrho)t^\delta}{\Gamma(\delta+1)} + \frac{16\tanh^3(\varrho)\operatorname{sech}^2(\varrho)t^\delta}{\Gamma(\delta+1)} \\
 &+ \frac{2\sin^2(\varrho)\tanh(\varrho)\operatorname{sech}^2(\varrho)t^\delta}{\Gamma(\delta+1)} + \frac{7}{8} + \dots
 \end{aligned}
 \tag{26}$$

The exact solutions are given by

$$\begin{aligned} u(\varrho, t) &= \tanh(\varrho + 2t) \cos\left(\varrho + \frac{17t}{8}\right), \\ v(\varrho, t) &= \tanh(\varrho + 2t) \sin\left(\varrho + \frac{17t}{8}\right), \\ w(\varrho, t) &= \frac{7}{8} - 2\tanh^2(\varrho + 2t). \end{aligned} \quad (27)$$

Note here that the first two solutions in the above system are periodic solutions, whereas the third one is a soliton solution. Thus, in our analysis, we use these solutions to check the effect of the fractional order on the profile of these solutions.

### 5. Numerical and Graphical Results

The profile of LRPSM solution  $u(\varrho, t)$  in both three- and two-dimensional form at different values of fractional order is introduced in Figure 1 by considering  $-4 \leq \varrho \leq 4$ ,  $0 \leq t \leq 1$ , and  $0 < \delta \leq 1$ . The wave profile, including its amplitude and width, is significantly influenced by the fractional order, as shown in Figure 1d. Moreover, the profile of LRPSM solution  $v(\varrho, t)$  in both three- and two-dimensional form at various values of fractional order with  $-3 \leq \varrho \leq 3$ ,  $0 \leq t \leq 1$ , and  $0 < \delta \leq 1$  is illustrated in Figure 2. One can see that the wave profile is shifted to behind the wave propagation with increasing fractional order. Moreover, the solitary wave solution  $w(\varrho, t)$  in both three- and two-dimensional form at different values of fractional order is considered, as illustrated in Figure 3. It is clear that the solitary wave amplitude decreases while the width increases with the enhancement in the fractional order, as elucidated in Figure 3d. Moreover, Table 1 illustrates the comparison of both the approximate solution  $u(\varrho, t)$  using LRPSM, the modified Laplace decomposition method (MLDM), and the exact solution, as well as the absolute error between them. The numerical findings demonstrate that the used method provides more accurate results when compared to other approximative methods. Table 2 introduces a comparison between the LRPSM solution  $v(\varrho, t)$  and the exact solution, as well as the absolute error between them. Furthermore, Table 3 illustrates the comparison between the LRPSM solution  $w(\varrho, t)$  and the exact solution and their absolute error. We can conclude that the used method is characterized by high accuracy compared to other approximate methods, and this reinforces its position in analyzing many complicated nonlinear evolution equations.

**Table 1.** Comparison of the  $u(\varrho, t)$  LRPSM solution and  $u(\varrho, t)$  exact solution along with absolute error (AE) using modified Laplace decomposition method (MLDM) and our present method.

$\varrho$	$u(\varrho, t)$ (LRPSM)	$u(\varrho, t)$ (Exact)	(AE) MLDM	(AE) Present Method
0	0.002	0.002	$3.32134 \times 10^{-7}$	$7.18227967 \times 10^{-9}$
0.1	0.101118	0.101118	$3.27273 \times 10^{-7}$	$4.63407702 \times 10^{-9}$
0.2	0.195239	0.195239	$3.18380 \times 10^{-7}$	$7.56282521 \times 10^{-8}$
0.3	0.279864	0.279864	$3.05178 \times 10^{-7}$	$2.19723957 \times 10^{-7}$
0.4	0.351214	0.351214	$2.87404 \times 10^{-7}$	$3.9217564 \times 10^{-7}$
0.5	0.406451	0.406451	$2.64809 \times 10^{-7}$	$5.13195369 \times 10^{-7}$
0.6	0.443772	0.443772	$2.37161 \times 10^{-7}$	$5.10202766 \times 10^{-7}$

**Table 2.** Comparison of the  $v(\varrho, t)$  LRPSM solution and  $v(\varrho, t)$  exact solution along with absolute error (AE) using modified Laplace decomposition method (MLDM) and our present method.

$\varrho$	$v(\varrho, t)$ (LRPSM)	$v(\varrho, t)$ (Exact)	(AE) MLDM	Abs. Present Method
0	$4.25 \times 10^{-6}$	$4.24999 \times 10^{-6}$	$8.86383 \times 10^{-7}$	$8.86522 \times 10^{-12}$
0.1	0.010363	0.010363	$1.78092 \times 10^{-7}$	$1.16606 \times 10^{-7}$
0.2	0.04001	0.040009	$2.77216 \times 10^{-7}$	$4.06303 \times 10^{-7}$
0.3	0.087225	0.087224	$3.85756 \times 10^{-7}$	$7.30429 \times 10^{-7}$
0.4	0.149373	0.149372	$5.03436 \times 10^{-7}$	$9.40811 \times 10^{-7}$
0.5	0.223169	0.223168	$6.29958 \times 10^{-7}$	$9.48364 \times 10^{-7}$
0.6	0.304988	0.304987	$7.65000 \times 10^{-7}$	$7.51894 \times 10^{-7}$

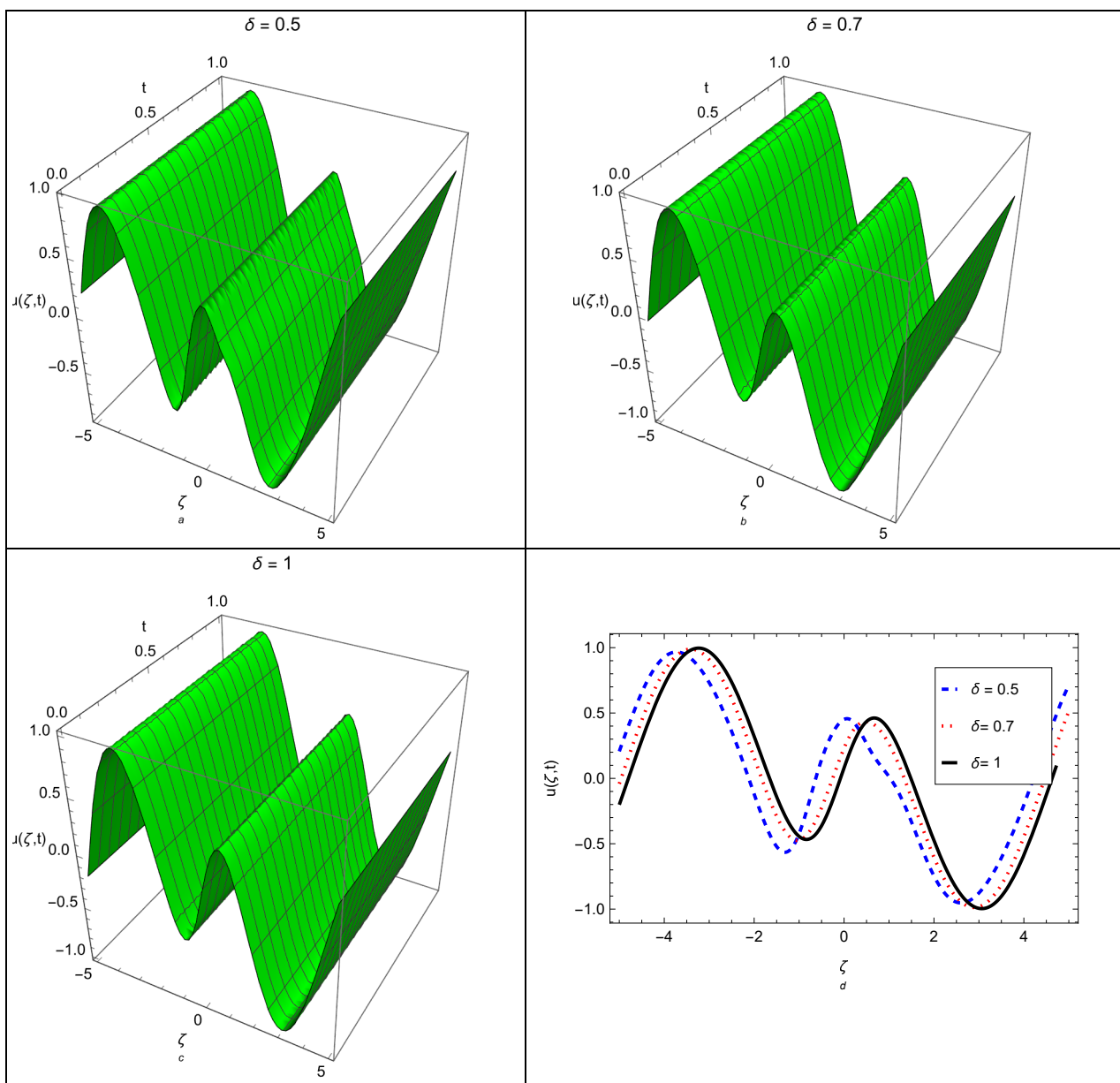


**Figure 1.** The profile of LRPSM periodic solution  $u(\varrho, t)$  in (a–c) three-dimensional and (d) two-dimensional form, at different values of fractional order.

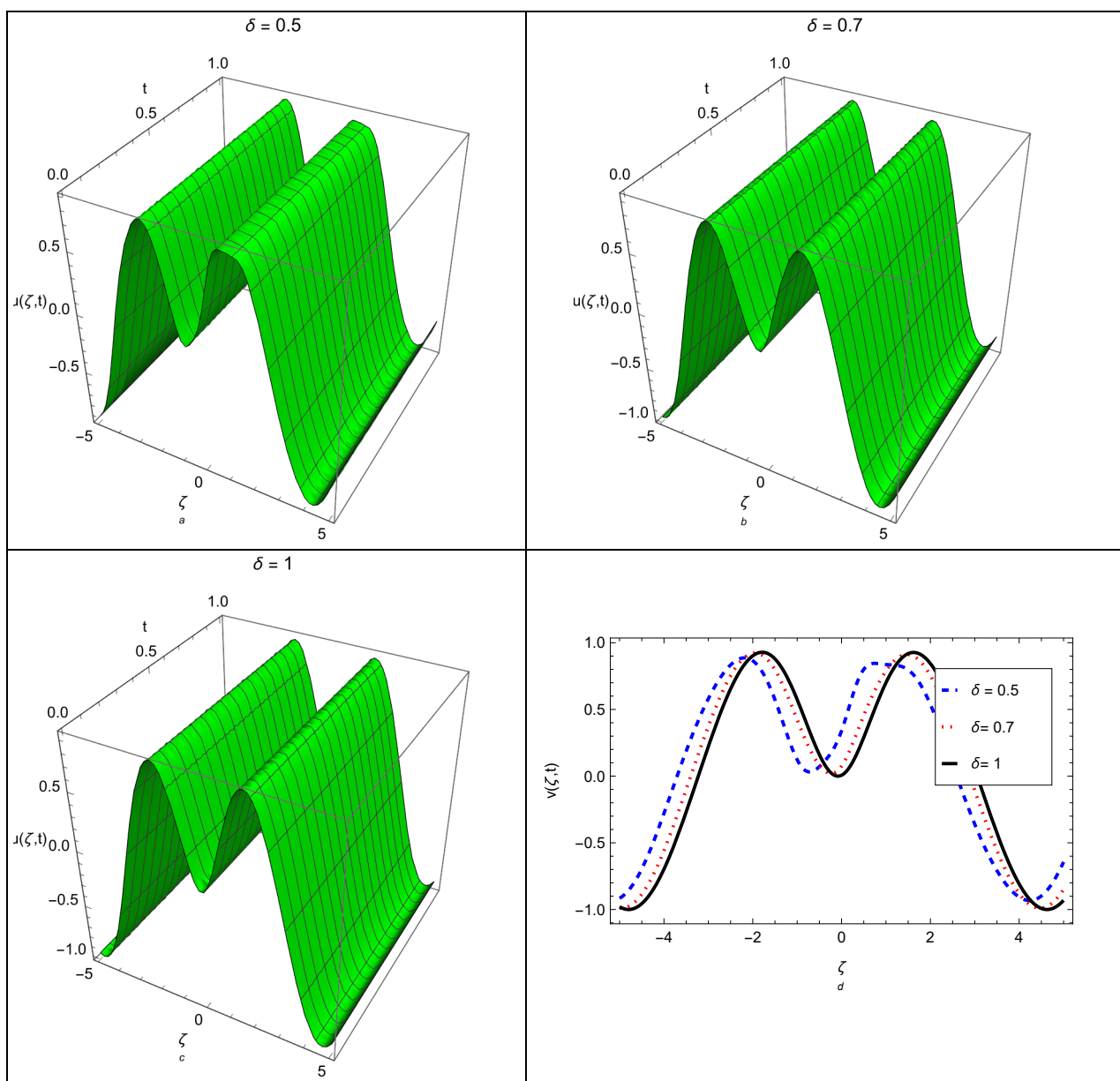


**Figure 2.** The profile of LRPSM periodic solution  $v(\eta, t)$  in (a–c) three-dimensional and (d) two-dimensional form, at different values of fractional order.

**Table 3.** Comparison of the  $w(\eta, t)$  LRPSM solution and  $w(\eta, t)$  exact solution along with their corresponding absolute error (AE).

$\eta$	$w(\eta, t)(LRPSM)$	$w(\eta, t)(Exact)$	Abs. Present Method
0.1	0.855102	0.855125	$2.3172 \times 10^{-5}$
0.2	0.797029	0.797071	$4.16755 \times 10^{-5}$
0.3	0.7052	0.705253	$5.21771 \times 10^{-5}$
0.4	0.586198	0.586252	$5.34746 \times 10^{-5}$
0.5	0.44782	0.447866	$4.6502 \times 10^{-5}$
0.6	0.298091	0.298125	$3.36853 \times 10^{-5}$
0.7	0.14443	0.144448	$1.80268 \times 10^{-5}$

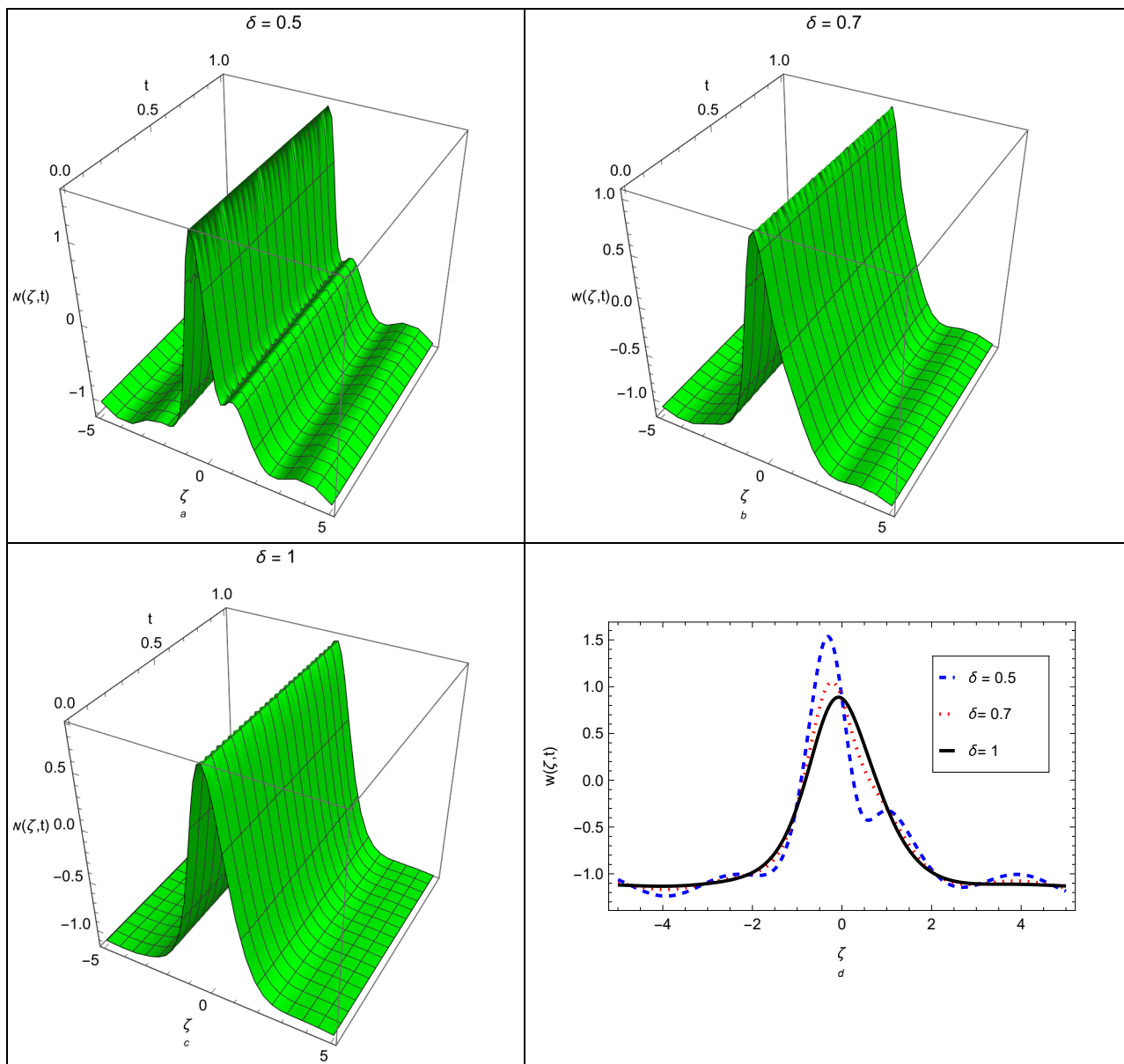


**Figure 3.** The profile of LRPSM soliton solution  $w(\zeta, t)$  in (a–c) three-dimensional and (d) two-dimensional form, at different values of fractional order.

## 6. Conclusions

This study focused on the investigation of the fractional-order Schrödinger–KdV (S-KdV) equation with the Caputo operator using the Laplace residual power series method. The equation accounts for memory effects and non-local behavior by incorporating the Caputo operator and fractional derivatives, bridging the divide between nonlinear dynamics and quantum mechanics. In solving fractional differential equations, the Laplace residual power series method proved to be an effective and precise numerical technique. Various facets of the fractional S-KdV equation, including the fractional order and initial conditions, were investigated using exhaustive numerical simulations. The findings enhance our comprehension of the complex interaction between quantum mechanics and nonlinear dynamics in fractional systems, casting light on wave phenomena and soliton solutions in these equations. In addition, the proposed method demonstrates its efficacy as a computational instrument for the analysis of complex physical systems involving fractional calculus and the Caputo operator. This research contributes to the greater comprehension of fractional differential equations and their applications in various scientific fields.

**Author Contributions:** Methodology, S.N.; Validation, B.M.A.; Formal analysis, R.S. and S.M.E.I.; Investigation, S.A.E.-T.; Resources, S.N. and R.S.; Data curation, S.A.E.-T.; Funding acquisition, S.N. All authors have read and agreed to the published version of the manuscript.

**Funding:** The authors express their gratitude to Princess Nourah bint Abdulrahman University Researchers Supporting Project number (PNURSP2023R32), Princess Nourah bint Abdulrahman University, Riyadh, Saudi Arabia. This work was supported by the Deanship of Scientific Research, the Vice Presidency for Graduate Studies and Scientific Research, King Faisal University, Saudi Arabia (Grant No. 3922).

**Data Availability Statement:** The numerical data used to support the findings of this study are included within the article. Mathematica codes for drawing the figures are available, which can be requested from El-Tantawy.

**Acknowledgments:** The authors express their gratitude to Princess Nourah bint Abdulrahman University Researchers Supporting Project number (PNURSP2023R32), Princess Nourah bint Abdulrahman University, Riyadh, Saudi Arabia. This work was supported by the Deanship of Scientific Research, the Vice Presidency for Graduate Studies and Scientific Research, King Faisal University, Saudi Arabia (Grant No. 3922).

**Conflicts of Interest:** The authors declare that there are no conflict of interest regarding the publication of this article.

## References

1. Noor, S.; Hammad, M.M.; Shah, R.; Alrowaily, A.W.; El-Tantawy, S.A. Numerical Investigation of Fractional-Order Fornberg–Whitham Equations in the Framework of Aboodh Transformation. *Symmetry* **2023**, *15*, 1353. [\[CrossRef\]](#)
2. Yasmin, H.; Abu Hammad, M.M.; Shah, R.; Alotaibi, B.M.; Ismaeel, S.M.; El-Tantawy, S.A. On the Solutions of the Fractional-Order Sawada–Kotera–Ito Equation and Modeling Nonlinear Structures in Fluid Mediums. *Symmetry* **2023**, *15*, 605. [\[CrossRef\]](#)
3. Kilbas, A.A.; Srivastava, H.M.; Trujillo, J.J. *Theory and Applications of Fractional Differential Equations*; Elsevier: Amsterdam, The Netherlands, 2006.
4. Baleanu, D.; Guevenc, Z.B.; Tenreiro, Machado, J.A. *New Trends in Nanotechnology and Fractional Calculus Applications*; Springer: New York, NY, USA, 2010.
5. Caputo, M. *Elasticita e Dissipazione*; Zanichelli: Bologna, Italy, 1969.
6. Riemann, G.F.B. *Versuch Einer Allgemeinen Auffassung der Integration und Differentiation*; Gesammelte Mathematische Werke: Leipzig, Germany, 1896.
7. Liouville, J. Memoire sur quelques questions de geometrie et de mecanique, et sur un nouveaugenre de calcul pour resoudre ces questions. *J. Ec. Polytech.* **1832**, *13*, 1–69.
8. Podlubny, I. *Fractional Differential Equations*; Academic Press: New York, NY, USA, 1999.
9. Miller, K.S.; Ross, B. *An Introduction to Fractional Calculus and Fractional Differential Equations*; Wiley: New York, NY, USA, 1993.
10. Li, Y.; Liu, F.; Turner, I.W.; Li, T. Time-fractional diffusion equation for signal smoothing. *Appl. Math. Comput.* **2018**, *326*, 108–116. [\[CrossRef\]](#)
11. Lin, W. Global existence theory and chaos control of fractional differential equations. *J. Math. Anal. Appl.* **2007**, *332*, 709–726. [\[CrossRef\]](#)
12. Veerasha, P.; Prakasha, D.G.; Baskonus, H.M. Solving smoking epidemic model of fractional order using a modified homotopy analysis transform method. *Math. Sci.* **2019**, *13*, 115–128. [\[CrossRef\]](#)
13. Wang, B.; Zhang, Y.; Zhang, W. A Composite Adaptive Fault-Tolerant Attitude Control for a Quadrotor UAV with Multiple Uncertainties. *J. Syst. Sci. Complex.* **2022**, *35*, 81–104. [\[CrossRef\]](#)
14. Xie, X.; Huang, L.; Marson, S.M.; Wei, G. Emergency response process for sudden rainstorm and flooding: Scenario deduction and Bayesian network analysis using evidence theory and knowledge meta-theory. *Nat. Hazards* **2023**, *117*, 3307–3329. [\[CrossRef\]](#)
15. Zhu, H.; Xue, M.; Wang, Y.; Yuan, G.; Li, X. Fast Visual Tracking with Siamese Oriented Region Proposal Network. *IEEE Signal Process. Lett.* **2022**, *29*, 1437. [\[CrossRef\]](#)
16. Meng, Q.; Ma, Q.; Shi, Y. Adaptive Fixed-time Stabilization for a Class of Uncertain Nonlinear Systems. *IEEE Trans. Autom. Control* **2023**, 1–8. [\[CrossRef\]](#)
17. Zhong, Q.; Han, S.; Shi, K.; Zhong, S.; Kwon, O. Co-Design of Adaptive Memory Event-Triggered Mechanism and Aperiodic In-termittent Controller for Nonlinear Networked Control Systems. *IEEE Trans. Circuits Syst. II Express Briefs* **2022**, *69*, 4979–4983. [\[CrossRef\]](#)
18. Guo, C.; Hu, J. Fixed-Time Stabilization of High-Order Uncertain Nonlinear Systems: Output Feedback Control Design and Settling Time Analysis. *J. Syst. Sci. Complex.* **2023**, 1–22. [\[CrossRef\]](#)
19. Guo, C.; Hu, J. Time base generator based practical predefined-time stabilization of high-order systems with unknown disturbance. *IEEE Trans. Circuits Syst. II Express Briefs* **2023**. [\[CrossRef\]](#)

20. Alhejaili, W.; Douanla, D.V.; Alim, A.; Tiofack, C.G.; Mohamadou, A.; El-Tantawy, S.A. Multidimensional dust-acoustic rogue waves in electron-depleted complex magnetoplasmas. *Phys. Fluids* **2023**, *35*, 063102.
21. Mouhammadoul, B.B.; Alim, A.; Tiofack, C.G.; Mohamadou, A.; Alrowaily, A.W.; Ismaeel, S.; El-Tantawy, S.A. On the super positron-acoustic rogue waves in q-nonextensive magnetoplasmas. *Phys. Fluids* **2023**, *35*, 054109.
22. El-Tantawy, S.A.; Salas, A.H.; Alyousef, H.A.; Alharthi, M.R. Novel approximations to a nonplanar nonlinear Schrödinger equation and modeling nonplanar rogue waves/breathers in a complex plasma. *Chaos Solitons Fractals* **2023**, *163*, 112612. [[CrossRef](#)]
23. El-Tantawy, S.A.; Alharbey, R.A.; Salas, A.H. Novel approximate analytical and numerical cylindrical rogue wave and breathers solutions: An application to electronegative plasma. *Chaos Solitons Fractals* **2022**, *155*, 111776. [[CrossRef](#)]
24. Albalawi, W.; El-Tantawy, S.A.; Salas, A.H. On the rogue wave solution in the framework of a Korteweg–de Vries equation. *Results Phys.* **2021**, *30*, 104847. [[CrossRef](#)]
25. El-Tantawy, S.A.; Alshehri, M.H.; Duraihem, F.Z.; El-Sherif, L.S. Dark soliton collisions and method of lines approach for modeling freak waves in a positron beam plasma having superthermal electrons. *Results Phys.* **2020**, *19*, 103452. [[CrossRef](#)]
26. Hasegawa, A.; Tappert, F. Transmission of stationary nonlinear optical pulses in dispersive dielectric fibers. I. Anomalous dispersion. *Appl. Phys. Lett.* **1973**, *23*, 142–144. [[CrossRef](#)]
27. Zakharov, V.E.; Shabat, A.B. Exact theory of two-dimensional self-focusing and one-dimensional self-modulation of waves in nonlinear media. *Sov. Phys. JETP* **1972**, *34*, 62–69.
28. Fan, E. Multiple travelling wave solutions of nonlinear evolution equations using a unified algebraic method. *J. Phys. A Math. Gen.* **2002**, *35*, 6853. [[CrossRef](#)]
29. Kucukarslan, S. Homotopy perturbation method for coupled schrödinger-KdV equation. *Nonlinear Anal. Real World Appl.* **2009**, *10*, 2264–2271. [[CrossRef](#)]
30. Triki, H.; Biswas, A. Dark solitons for a generalized nonlinear Schrödinger equation with parabolic law and dual power nonlinearity. *Math. Methods Appl. Sci.* **2011**, *34*, 958–962. [[CrossRef](#)]
31. Zhang, L.H.; Si, J.G. New soliton and periodic solutions of (1+2)-dimensional nonlinear Schrödinger equation with dual power nonlinearity. *Commun. Nonlinear Sci. Numer. Simul.* **2010**, *15*, 2747–2754. [[CrossRef](#)]
32. Biswas, A. A perturbation of solitons due to power law nonlinearity. *Chaos Solitons Fractals* **2001**, *12*, 579–588. [[CrossRef](#)]
33. JBronski, C.; Carr, L.D.; Deconinck, B.; Kutz, J.N. Bose-Einstein condensates in standing waves: The cubic nonlinear Schrödinger equation with a periodic potential. *Phys. Rev. Lett.* **2001**, *86*, 1402–1405. [[CrossRef](#)]
34. Nore, C.; Brachet, M.E.; Fauve, S. Numerical study of hydrodynamics using the nonlinear Schrödinger equation. *Phys. D Nonlinear Phenom.* **1993**, *65*, 154–162. [[CrossRef](#)]
35. Eslami, M.; Mirzazadeh, M. Topological 1-soliton of nonlinear Schrödinger equation with dual power nonlinearity in optical fibers. *Eur. Phys. J. Plus* **2013**, *128*, 141–147. [[CrossRef](#)]
36. Albalawi, W.; Shah, R.; Nonlaopon, K.; El-Sherif, L.S.; El-Tantawy, S.A. Laplace Residual Power Series Method for Solving Three-Dimensional Fractional Helmholtz Equations. *Symmetry* **2023**, *15*, 194. [[CrossRef](#)]
37. Li, C.; Qian, D.; Chen, Y. On Riemann-Liouville and caputo derivatives. *Discret. Dyn. Nat. Soc.* **2011**, *2011*, 562494. [[CrossRef](#)]
38. Kexue, L.; Jigen, P. Laplace transform and fractional differential equations. *Appl. Math. Lett.* **2011**, *24*, 2019–2023. [[CrossRef](#)]
39. He, H.M.; Peng, J.G.; Li, H.Y. Iterative approximation of fixed point problems and variational inequality problems on Hadamard manifolds. *UPB Bull. Ser. A* **2022**, *84*, 25–36.
40. Arqub, O.A.; El-Ajou, A.; Momani, S. Constructing and predicting solitary pattern solutions for nonlinear time-fractional dispersive partial differential equations. *J. Comput. Phys.* **2015**, *293*, 385–399. [[CrossRef](#)]
41. Alaroud, M. Application of Laplace residual power series method for approximate solutions of fractional IVP's. *Al-Exandria Eng. J.* **2022**, *61*, 1585–1595. [[CrossRef](#)]
42. Yavuz, M.; Sulaiman, T.A.; Yusuf, A.; Abdeljawad, T. The Schrödinger-KdV equation of fractional order with Mit-tag-Leffler nonsingular kernel. *Alex. Eng. J.* **2021**, *60*, 2715–2724. [[CrossRef](#)]

**Disclaimer/Publisher's Note:** The statements, opinions and data contained in all publications are solely those of the individual author(s) and contributor(s) and not of MDPI and/or the editor(s). MDPI and/or the editor(s) disclaim responsibility for any injury to people or property resulting from any ideas, methods, instructions or products referred to in the content.